RESEARCH ARTICLE

Multiple dynamics in a delayed predator-prey model with asymmetric functional and numerical responses

Bapan Ghosh[1] | **Binandita Barman**[2,3] | **Manideepa Saha**[3]

[1]Differential Equations, Modeling, and Simulation Group, Department of Mathematics, Indian Institute of Technology Indore, Simrol, Indore, 453552, Madhya Pradesh, India

[2]Department of Mathematics, Goalpara College, Goalpara, 783101, Assam, India

[3]Department of Mathematics, National Institute of Technology Meghalaya, Shillong, 793003, Meghalaya, India

Correspondence
Bapan Ghosh, Differential Equations, Modeling, and Simulation Group, Department of Mathematics, Indian Institute of Technology Indore, Simrol, Indore, Madhya Pradesh 453552, India.
Email: keshab.bapan@iiti.ac.in

Communicated by: R. Bravo de la Parra

We consider a predator-prey model with dissimilar functional and numerical responses that induce an Allee effect. There is a time lag between consumption and digestion of prey biomass by predator. Hence, a time delay has been incorporated in the numerical response function. The system consists of two interior equilibria. Taking time delay as the bifurcation parameter, four different dynamic behaviors appear, viz., (R1) system undergoes no change in its stability for all time delay, (R2) system undergoes stability change, (R3) system undergoes stability switching, and (R4) system undergoes instability switching. Here, finding four distinct dynamics in a single population model with only one delay is a novelty in this contribution. This variation in dynamics emerges due to asymmetricity in functional and numerical responses. All the relevant theorems in establishing stability are provided, and these are verified numerically. We analytically prove that if an interior equilibrium is a saddle point in absence of time delay, then the equilibrium cannot be stabilized by varying the time delay. It is popularly believed that existence of two distinct pair of purely imaginary roots of the characteristic function leads to stability switching. However, we provide examples where the system remains unstable, stability changes, and instability switching occurs. This is another new and interesting observation in our work. The numerical examples are furnished with phase portraits, time series plots, bifurcation diagrams, and eigenvalues evaluation with delay, for better understanding. Our model with a single delay exhibits variety of dynamics, which were not explored before.

KEYWORDS
Allee effect, eigenvalues, instability switching, population dynamics, saddle point

MSC CLASSIFICATION
34K18, 34K20, 92B05

1 | INTRODUCTION

Numerous mathematical models of population dynamics have been developed by researchers across the world to analyze the various behaviors that the species can portray in the environment. Several literature have studied the factors that

impacted the dynamic behavior of predator and prey in nature. It has been established that the stability of predator-prey models is effected by Allee effect,[1,2] predator interference,[3] foraging facilitation,[4] population harvesting,[5] fear effect,[6] presence of intra-specific competition,[7] time delays,[8–10] etc.

Time delays in any predator-prey model are incorporated due to various factors like delays in growth of the species due to its gestation and maturation,[11,12] delay in consumption of prey by predator,[13,14] delay in dispersal from one patch to another,[15] etc. Time delays largely affect the stability of ecological models. For instance, Collera[16] has studied an intraguild predator-prey system with time delay in the logistic growth of basal resource. He concluded that time delay has a destabilizing nature. Similar conclusion was derived by Rabago and Collera[17] in their delayed intraguild predator-prey model. Zhang et al.[18] have considered a predator-prey model where time delay is due to the gestation of predator. They found that periodic solutions are possible when time delay is varied, i.e., predator coexists with the prey in an oscillatory mode. A three time delayed predator-prey model was discussed by Jiang and Wang.[19] They proved the existence of global periodic solutions. Lately, Pati and Ghosh[20] have studied a predator-prey model with a single time delay in the logistic growth of prey. They inferred possibility of three types of stability scenarios at the coexisting equilibrium, viz., no change in stability, stability change from stable to unstable, and stability switching. They also detected the existence of delay induced supercritical, subcritical, and non-degenerate Hopf bifurcations around the interior equilibrium. Singh et al.[21] have studied a predator-prey model with two discrete time delays in the logistic term of prey and the numerical response of predator. Various possible dynamics including switching of stability and existence of limit cycles are shown to occur for the system. The case of bistability also exists in predator-prey model when time delay is incorporated in the fear effect of prey due to predator.[22] Kumar and Sharma[23] have considered a population model of senior players and new players in any sports. They proved that time delay due to age gap of the players in the intra-specific competition among the players can destabilize even a globally stable interior equilibrium.

Another factor that effects the predator-prey dynamics greatly is the Allee effect arising due to reasons like increase in predation, social dysfunction, etc. Allee effects may be defined by the positive correlation between per capita growth rate of a population and small population sizes. Allee effects are categorized as strong and weak Allee effects. In case of strong Allee effect, the population could become extinct if the initial species density is below a threshold level. However, the weak Allee effect does not induce species extinction, but the dynamic solutions take relatively longer time to reach the positive equilibrium state. A comprehensive study could be found in Drake and Kramer.[24] Several impacts due to presence of Allee effect are explained by Zu and Mimura.[25] They reported that when Allee effect of prey species is strong, it can lead to extinction of prey and predator. It can even induce unstable periodic oscillation in the system. The combined impacts of both time delays and Allee effects are studied worldwide to understand the dynamics both the factors display. A delayed model of predator and prey (with Allee effect) has been investigated by Anacleto and Vidal[26] to show the existence of stability switching analytically and establish the direction of Hopf-bifurcation with respect to time delay. They have found that the delay due to the gestation period can be effected by Allee effect, leading to a stability switching around the coexisting equilibrium. Xiao et al.[27] have incorporated time delay in the numerical response of predator and an Allee effect in the logistic growth of prey. They found that the system undergoes Hopf bifurcation, when time delay is the bifurcation parameter. They also determined that both the species become extinct due to larger Allee effect. On the other hand, in the predator-prey model by Anacleto and Vidal,[26] the growth term of the prey is effected by both time delay due to maturation as well as by Allee effect. It was observed that Allee effect plays an important role in the existence of positive eqilibria. Stability change and stability switching occur as a consequence of time delay. Usually in the above mentioned literature, it is found that Allee effect and time delays are destabilizing in nature. However, it is not always the case. Vinoth et al.[28] have shown the stabilizing nature of Allee effect and gestation delay in a tri-trophic food chain model. Tao and Zhu[29] have considered a diffusion-reaction predator-prey model with time delay and Allee effect. They found that the time delay and Allee effect have a potential role to play in the formation of Turing pattern. Thus, we can draw to a conclusion that in all the literature, factors like the Allee effect and time delay play a significant role in changing the system dynamics.

In this contribution, we report a class of new dynamics that arises in a predator-prey model under the combined effect of time delay and Allee effect. In the next section, we detail our motivation for studying the research theme and model selection. In the succeeding section, the positivity and boundedness of the proposed model are discussed. In Section 4, stability analysis of the system is investigated corresponding to the equilibria. Several analytical theory along with numerical examples are presented, and their validations are performed. Final section presents the summary of the study and future research perspective.

2 | MOTIVATION AND MODEL FORMULATION

Wangersky and Cunningham[30] were the pioneer to have introduced time lag in the predation process in a Lotka-Voltera type predator-prey model with finite carrying capacity for prey. They found that the solution of the predator-prey model depends upon the time delay parameter. The same Wangersky-Cunningham (WC) predator-prey model subjected to constant-rate prey harvesting was studied by Martin and Ruan.[31] They considered the WC model, which is equivalent to the following system:

$$\dot{x}(t) = rx(t)\left(1 - \frac{x(t)}{K}\right) - \alpha x(t)y(t) - H,$$
$$\dot{y}(t) = \beta x(t-\tau)y(t-\tau) - my(t),$$
(1)

where $x(\theta) > 0$, $y(\theta) > 0$ and are continuous on $\theta \in [-\tau, 0]$. Here, $x(t)$ and $y(t)$ are the prey and predator population biomass, respectively, at time t. The time delay τ is incorporated in the predator numerical response. Here, r denotes the intrinsic growth rate of the prey, and K is the carrying capacity of the prey. The attack rate during predation is denoted by α and $\beta = \alpha a$, where a is conversion coefficient of prey biomass into predator. We define m as the specific mortality rate of predator, and H is the constant-rate harvesting of the prey. Martin and Ruan[31] reported three types of dynamics for the system (1) when time delay increases, viz., **(R1)**: The system remains stable for all time delay τ; **(R2)**: A stable equilibrium in the system becomes unstable for increase in time delay and cannot change its stability; and **(R3)**: The system experiences a finite number of stability switching. The first two results **(R1)** and **(R2)** are verified numerically by Martin and Ruan,[31] but validity of **(R3)** is neither proved analytically nor numerically. This rises a question whether switching of stability is exhibited in their model.

Very interestingly, Toaha[32] also considered the Wangersky-Cunningham (WC) model linked with linear harvesting term, which is similar to

$$\dot{x}(t) = rx(t)\left(1 - \frac{x(t)}{K}\right) - \alpha x(t)y(t) - Ex(t),$$
$$\dot{y}(t) = \beta x(t-\tau)y(t-\tau) - my(t) - Ey(t),$$
(2)

where E is the combined (equal) harvesting effort. He established that two distinct dynamics, viz., **(R1)** and **(R2)** hold in the WC model. Analytically, it was proved that the third result **(R3)** is impossible to occur.

Recently, Barman and Ghosh[7] have also found that the first two dynamical behaviors (**R1-R2**) are possible in a class of four predator-prey models, when time delay is incorporated in the numerical response. They have analytically proved that the first result **(R1)** is possible only when the intra-specific competition is present among predators; otherwise, a stability change must happen for increasing delay. This leads to a question if the intra-specific competition induces stability switching in other population dynamics models. It motivates us to study WC model incorporating intra-specific competition among predators. We first consider the WC model with intra-specific competition in predator, which reads as

$$\dot{x}(t) = rx(t)\left(1 - \frac{x(t)}{K}\right) - \alpha x(t)y(t),$$
$$\dot{y}(t) = \beta x(t-\tau)y(t-\tau) - my(t) - \gamma y^2(t),$$
(3)

where γ is the intra-specific competition coefficient. The stability analysis of the system (3) in the presence of intra-specific competition is supplied in Appendix A1. Our analytical results report that switching of stability **(R3)** does not occur. It is found that intra-specific competition has no role in inducing stability switching. The dynamical behaviors of system (3) are on par with the outcomes of system (2) studied by Toaha.[32]

Li and Takeuchi[14] have studied a predator-prey model with Beddington-DeAngelis functional response and intra-specific competition among predators. The delay was incorporated in the predator response term. They discussed the parameteric conditions under which all three results **(R1–R3)** hold. On the other hand, Ye et al.[33] have considered a predator-prey model with weak Allee effect in prey growth and incorporated searching as well as digestion delay in their interaction terms. It is found that results **(R1–R3)** hold true in their model when both the delay terms are non-zero. When one of the delay is zero, the first two results **(R1–R2)** hold true. Therefore, based on the above studies, it is clear that switching does not exhibit for a single delay in predation process in predator-prey system. Also, no situations occurred where all the three cases **(R1–R3)** are validated when the single time delay τ is the bifurcating parameter. This motivates

us to investigate for the existence of a predator-prey system which exhibits all the possible dynamics, viz., **(R1–R3)**. Further, we also want to examine the validity of **(R4)**: an unstable equilibrium changes its stability and regains its instability, i.e., whether instability switching arises in the same system due to increase in delay. Thus, we consider a predator-prey model with Holling type I functional response subject to Allee effect in the predator as follows:

$$
\begin{aligned}
\dot{x}(t) &= rx(t)\left(1 - \frac{x(t)}{K}\right) - \alpha x(t)y(t), \\
\dot{y}(t) &= \beta x(t-\tau)y(t-\tau)\left(\frac{y(t-\tau)}{C+y(t-\tau)}\right) - my(t) - \gamma y^2(t),
\end{aligned}
\tag{4}
$$

where C is the Allee effect constant. The functional response represents the consumption of the prey biomass by predator. However, the digestion of the prey biomass by the predator is not instanteneous. It takes some time. Henceforth, a delay τ has been incorporated in the numerical response, which depends on the previous prey and predator biomass at time $(t-\tau)$. We have considered the same delay τ in the numerical response $\beta x(t-\tau)y(t-\tau)\frac{y(t-\tau)}{C+y(t-\tau)}$. The representation of same τ in our model is influenced by the delayed Gause-type predator-prey model (System 1.4) in Martin and Ruan.[31] The change rate of the predator population depends on the number of prey and of predators existing at some previous time. Note that the functional response and numerical response are not proportional to each other due to the presence of Allee effect. It can be seen that in absence of the Allee effect constant C, system (4) turns into system (3). Zhou et al.[34] have incorporated similar Allee effect terms in the predator population of the classical Lotka-Volterra predator-prey model. It was observed that the dynamics of the Lotka-Volterra model changes from neutrally stable mode to unstable mode due to the Allee effect in the predator. The larger Allee effect constant slows down the growth rate of the predator. In Verdy,[1] the Allee effect was found to modulate the predation rate. Bajeux et al.[35] have discussed about biological control tactics in a predator-prey model in which two component Allee effects are present, viz., foraging efficiency and reproductive Allee effects. Costa and dos Anjos[36] have incorporated reproductive Allee effect in the Rosenzweig-MacArthur predator-prey model with intra-specific competition among predators. Bistability and Hydra effect in the system were observed when mortality rate increased. We incorporate an Allee effect among predators' numerical response considered by Zhou et al.,[34] Bajeux et al.,[35] and Costa et al.[37] to examine whether all the delay induced dynamics **(R1–R4)** are observed.

3 | POSITIVITY AND BOUNDEDNESS

Before proceeding to investigate the validness of the results **R1–R4** for (4), we first verify the positivity and boundedness of its solutions.

Theorem 3.1. *The solutions of system (4) are positive for $t > 0$ with given initial conditions $x(\theta) > 0$, $y(\theta) > 0$, where $\theta \in [-\tau, 0]$.*

Proof. We need to show that for any time $t > 0, x(t) > 0,$ and $y(t) > 0$. Let us first show that $x(t) > 0$. The solution of the first equation of system (4) can be written as

$$
x(t) = x(0)e^{\int_0^t \left\{r - \frac{rx(s)}{K} - \alpha y(s)\right\}ds} > 0.
$$

Now, for $t > 0$, we show that $y(t) > 0$. Suppose that there exists a time $t = t_1 > 0$ such that $y(t_1) = 0$ and $y(t) > 0$ for $t \in [0, t_1)$. Then, for $t \in (0, t_1), x(t-\tau) > 0,$ and $y(t-\tau) > 0$. Hence,

$$
\dot{y}(t) > -my(t) - \gamma y^2(t), \ t \in (0, t_1).
$$

So by standard comparison theorem, we can write

$$
y(t) > y(0)e^{\int_0^t \{-m - \gamma y(s)\}ds}.
$$

Since $y(t)$ is continuous on $[0, t_1)$, there exists $Y > 0$ such that $y(t) < Y$ for $t \in [0, t_1]$. Thus,

$$y(t) > y(0)e^{\int_0^t \{-m - \gamma Y\} ds} \text{ for } t \in [0, t_1).$$

This implies $y(t_1) > 0$, as $y(t)$ is continuous on $[0, t_1]$, which is a contradiction to the fact that $y(t_1) = 0$. Thus, the prey and predator populations remain positive for all time. □

Second, we establish that the prey and predator populations are bounded for all time.

Theorem 3.2. *The solutions of system (4) are bounded for $t > 0$ with given initial conditions $x(\theta) > 0$, $y(\theta) > 0$, where $\theta \in [-\tau, 0]$.*

Proof. Since $x(t) > 0$, $\forall\, t > 0$, we can write

$$\dot{x}(t) \leq rx(t)(1 - x(t)/K).$$

This signifies that

$$\lim_{t \to +\infty} \sup x(t) \leq K.$$

This implies, for any $\epsilon > 0$, there exists $T > 0$ such that $0 < x(t) \leq K + \epsilon$ for $t \geq T$. Thus, for $t \geq T$, we get

$$\beta \dot{x}(t) + \alpha \dot{y}(t + \tau) = r\beta x(t)(1 - x(t)/K) - m\alpha y(t + \tau)$$
$$+ \alpha\beta x(t)y(t)\left(\frac{y(t)}{C + y(t)}\right) - \alpha\beta x(t)y(t) - \gamma\alpha y^2(t + \tau)$$
$$\leq r\frac{\beta}{K}x(t)(K - x(t)) - m\alpha y(t + \tau)$$
$$\leq \frac{r\beta K}{4} + \beta m(K + \epsilon) - \beta mx(t) - m\alpha y(t + \tau)$$
$$\left[\text{since } x(t)(K - x(t)) \leq \frac{K^2}{4}\right]$$
$$= \frac{r\beta K}{4} + \beta m(K + \epsilon) - m\{\beta x(t) + \alpha y(t + \tau)\}.$$

For ϵ arbitrarily small, $\lim_{t \to +\infty} \sup\{\beta x(t) + \alpha y(t + \tau)\} \leq \frac{r\beta K}{4m} + \beta K = M$. Henceforth, $\lim_{t \to +\infty} \sup y(t) \leq M/\alpha$. □

4 | MODEL ANALYSIS

In this section, at first, the equilibrium points of system (4) are determined. The trivial equilibrium $(0, 0)$ and boundary equilibrium $(K, 0)$ always exist for system (4). We now analyze the existence of interior steady state (x^*, y^*). The interior equilibrium must satisfy the equations:

$$r\left(1 - \frac{x^*}{K}\right) - \alpha y^* = 0, \tag{5}$$

$$\beta x^*\left(\frac{y^*}{C + y^*}\right) - m - \gamma y^* = 0. \tag{6}$$

From equations (5) and (6) we get,

$$x^* = \frac{K}{r}(r - \alpha y^*), \tag{7}$$

and

$$y^* = \frac{(\beta K - m - \gamma C) \pm \sqrt{(\beta K - m - \gamma C)^2 - 4mC\left(\frac{\beta K\alpha}{r} + \gamma\right)}}{2\left(\frac{\beta K\alpha}{r} + \gamma\right)}. \tag{8}$$

When both $C = \gamma = 0$, the unique interior equilibrium of the WC model is given as $(x^*, y^*) = \left(\frac{m}{\beta}, \frac{r(\beta K - m)}{\beta K \alpha} \right)$, provided $\beta K > m$.

In absence of C, the interior equilibrium of system (4) is given as $(x^*, y^*) = \left(K - K\alpha \frac{\beta K - m}{\beta K \alpha + \gamma r}, \frac{r(\beta K - m)}{\beta K \alpha + \gamma r} \right)$, provided $\beta K > m$. Therefore, the interior equilibrium of system (4) with $C = 0$ is always unique if it exists.

However, when $C > 0$, either there exists no interior equilibrium or two interior equilibria (x_1^*, y_1^*) and (x_2^*, y_2^*) exist only when $\beta K - \gamma C > m$ and $(\beta K - m - \gamma C)^2 > 4mC \left(\frac{\beta K \alpha}{r} + \gamma \right)$, where

$$x_1^* = \frac{K}{r}(r - \alpha y_1^*),$$

$$y_1^* = \frac{(\beta K - m - \gamma C) + \sqrt{(\beta K - m - \gamma C)^2 - 4mC \left(\frac{\beta K \alpha}{r} + \gamma \right)}}{2 \left(\frac{\beta K \alpha}{r} + \gamma \right)},$$

$$x_2^* = \frac{K}{r}(r - \alpha y_2^*),$$

and

$$y_2^* = \frac{(\beta K - m - \gamma C) - \sqrt{(\beta K - m - \gamma C)^2 - 4mC \left(\frac{\beta K \alpha}{r} + \gamma \right)}}{2 \left(\frac{\beta K \alpha}{r} + \gamma \right)}.$$

Now, we want to study the stability behavior of system (4) with respect to time delay.

The Jacobians J_0 and J_τ for system (4) corresponding to the interior equilibrium (x^*, y^*) are

$$J_0 = \begin{bmatrix} r - \frac{2rx^*}{K} - \alpha y^* & -\alpha x^* \\ 0 & -m - 2\gamma y^* \end{bmatrix}$$

and

$$J_\tau = \begin{bmatrix} 0 & 0 \\ \beta y^* \left(\frac{y^*}{y^* + C} \right) & \beta x^* \left(\frac{y^*}{y^* + C} + \frac{y^* C}{(y^* + C)^2} \right) \end{bmatrix}.$$

The characteristic equation corresponding to the linearized system of (4) is given as

$$\det \left(J_0 + J_\tau e^{-\lambda \tau} - \lambda I \right) = 0$$

$$\Rightarrow \begin{vmatrix} -\frac{rx^*}{K} - \lambda & -\alpha x^* \\ \beta y^* \left(\frac{y^*}{y^* + C} \right) e^{-\lambda \tau} & -(m + 2\gamma y^*) + \beta x^* \left(\frac{y^*(y^* + 2C)}{(y^* + C)^2} \right) e^{-\lambda \tau} - \lambda \end{vmatrix} = 0$$

$$\Rightarrow \lambda^2 + \left(\frac{rx^*}{K} + m + 2\gamma y^* \right) \lambda - \left(\beta x^* \frac{(y^*)^2 + 2Cy^*}{(y^* + C)^2} \right) \lambda e^{-\lambda \tau} +$$
$$\left(-\frac{rx^*}{K} \beta x^* \frac{(y^*)^2 + 2Cy^*}{(y^* + C)^2} + \alpha \beta x^* y^* \frac{y^*}{y^* + C} \right) e^{-\lambda \tau} + rx^* \frac{m + 2\gamma y^*}{K} = 0. \quad (9)$$

The characteristic equation can be further written as

$$\lambda^2 + a_1 \lambda + a_2 \lambda e^{-\lambda \tau} + a_3 + a_4 e^{-\lambda \tau} = 0, \quad (10)$$

where

$$a_1 = \frac{rx^*}{K} + m + 2\gamma y^*,$$

$$a_2 = -\beta x^* \frac{(y^*)^2 + 2Cy^*}{(y^* + C)^2},$$

$$a_3 = r\frac{x^*}{K}(m + 2\gamma y^*),$$

$$a_4 = -r\beta x^* \frac{x^*}{K} \frac{(y^*)^2 + 2Cy^*}{(y^* + C)^2} + \alpha\beta x^* \frac{(y^*)^2}{(y^* + C)}.$$

Note that the left side expression of characteristic equation (10) is the characteristic function. We first discuss the stability of the trivial equilibrium.

Result 4.1. *We find that irrespective of the value of τ, the trivial equilibrium have two roots of the characterictic function viz. r and -1. Thus, the trivial equilibrium is a saddle point (unstable).*

The stability of boundary equilibrium is discussed below:

Result 4.2. *The boundary equilibrium is locally stable for all τ since the characteristic function yields two negative roots $-r$ and $-m$ at the boundary equilibrium, independent of the value of τ.*

Now, we prove if this locally stable boundary equilibrium is globally stable under certain parameter condition.

Theorem 4.1. *The boundary equilibrium $(K, 0)$ is globally asymptotically stable whenever $\beta K < m$.*

Proof. We have proved that the solutions of system (4) are positive and bounded.
Hence,

$$\lim_{t\to+\infty} \sup x(t) \leq K.$$

So, for any positive ϵ, sufficiently small, there exists a $T = T(\epsilon)$ such that for $t > T$,

$$x(t) \leq K + \epsilon.$$

This shows that for $t > T + \tau$,

$$\dot{y}(t) \leq y(t - \tau)\beta(K + \epsilon)\frac{y(t - \tau)}{C + y(t - \tau)} - my(t)$$

$$\leq y(t - \tau)\beta(K + \epsilon) - my(t) \quad \left[\text{since } \frac{y(t - \tau)}{C + y(t - \tau)} \leq 1\right].$$

Thus, $\lim_{t\to+\infty} y(t) = 0$ whenever $\beta(K + \epsilon) < m$ (Lemma 4 of Shu et al.[38]). Now, for any $\delta > 0$, there exists a $T(\delta) > 0$ such that we have

$$\dot{x}(t) \geq x(t)\left(1 - \frac{x(t)}{K} - \alpha\delta\right),$$

which implies that $\lim_{t\to+\infty} \inf x(t) \geq K$. Since $\lim_{t\to+\infty} \sup x(t) \leq K$, thus $\lim_{t\to+\infty} x(t) = K$.[39, Proposition 1] Thus, $(K, 0)$ is globally asymptotically stable equilibrium point when $\beta K < m$. □

Now, we discuss the stability of the interior equilibria. For $\tau = 0$, the characteristic equation (10) reduces to

$$\lambda^2 + (a_1 + a_2)\lambda + (a_3 + a_4) = 0. \tag{11}$$

It is noticed from the characteristic equation (11) that in absence of delay, i.e., when $\tau = 0$, interior equilibrium $E = (x^*, y^*)$ is

1. locally stable (stable focus or node) if $a_1 + a_2 > 0$ and $a_3 + a_4 > 0$,
2. unstable (focus or node) if $a_1 + a_2 < 0$ and $a_3 + a_4 > 0$,
3. saddle point if $a_1 + a_2 > 0$ and $a_3 + a_4 < 0$.

In order to verify the change of stability in system (4), with time delay τ as the bifurcation parameter, there must exist a pair of eigenvalues $\lambda = \pm i\omega,\ (\omega > 0)$ of the characteristic equation (10). Now, substituting $\lambda = i\omega$ in equation (10) and separating the real and imaginary parts, we obtain

$$-\omega^2 + a_2\omega \sin \omega\tau + a_4 \cos \omega\tau + a_3 = 0, \tag{12}$$

$$a_1\omega + a_2\omega \cos \omega\tau - a_4 \sin \omega\tau = 0. \tag{13}$$

After eliminating τ from equations (12) and (13), we get

$$(\omega^2 - a_3)^2 + a_1^2\omega^2 = a_2^2\omega^2 + a_4^2,$$

which can be simplified as

$$\omega^4 + (a_1^2 - a_2^2 - 2a_3)\omega^2 - a_4^2 + a_3^2 = 0. \tag{14}$$

The roots of equation (14) are

$$\omega^2 = \frac{1}{2}(a_2^2 - a_1^2 + 2a_3) \pm \frac{1}{2}\left[(a_2^2 - a_1^2 + 2a_3)^2 - 4(a_3^2 - a_4^2)\right]^{1/2}. \tag{15}$$

We analyze the stability behavior of system (4) based on the roots of equation (14). From the right-side expression of equation (15), we obtain the following possible number of ω:

Case 1: If either $a_2^2 - a_1^2 + 2a_3 < 0$ and $a_3^2 - a_4^2 > 0$ or $(a_2^2 - a_1^2 + 2a_3)^2 < 4(a_3^2 - a_4^2)$, then there exists no positive ω.
Case 2: If $a_3^2 - a_4^2 < 0$, then there exists one positive ω denoted by ω_+.
Case 3: If $a_2^2 - a_1^2 + 2a_3 > 0$, $(a_2^2 - a_1^2 + 2a_3)^2 = 4(a_3^2 - a_4^2)$, then there exists a twofold positive ω.
Case 4: If $a_3^2 - a_4^2 > 0$, $a_2^2 - a_1^2 + 2a_3 > 0$ and $(a_2^2 - a_1^2 + 2a_3)^2 > 4(a_3^2 - a_4^2)$, then there exist two distinct positive ω denoted by ω_+ and ω_-, with $\omega_+ > \omega_-$.

We now find the critical τ corresponding to the positive ω. Solving equations (12) and (13), we get

$$\cos \omega\tau = \frac{(\omega^2 - a_3)a_4 - a_1a_2\omega^2}{a_2^2\omega^2 + a_4^2} =: C(\omega), \tag{16}$$

$$\sin \omega\tau = \frac{a_2\omega(\omega^2 - a_3) + a_1a_4\omega}{a_2^2\omega^2 + a_4^2} =: S(\omega). \tag{17}$$

Define $\theta_\pm = \arccos(C(\omega_\pm)) \in (0, \pi)$. The critical values $\tau_j^\pm$ of time delay τ (if exists) are obtained by substituting $\omega_\pm$ in equation (16) and are given as

$$\tau_j^\pm = \begin{cases} \frac{(2\pi - \theta_\pm)}{\omega_\pm} + \frac{2j\pi}{\omega_\pm}, & \text{if } S(\omega_\pm) < 0, \\ \frac{\theta_\pm}{\omega_\pm} + \frac{2j\pi}{\omega_\pm}, & \text{if } S(\omega_\pm) > 0, \quad j = 0, 1, 2, \ldots . \end{cases} \tag{18}$$

Remark 4.1. Existence of positive ω's corresponding to an equilibrium point may not change the stability in a system. We now demonstrate the fact through examples.

After acquiring the critical time delays, we examine if the eigenvalues on $\mathbb{C}^0$ (imaginary axis) change their signs when delay crosses the threshold values $\tau = \tau_j^\pm,\ j = 0, 1, 2, \ldots .$
Differentiating characteristic equation (10) w.r.t. τ, we obtain

$$\left(2\lambda + a_1 - a_2\lambda e^{-\lambda\tau}\tau + a_2 e^{-\lambda\tau} - a_4 e^{-\lambda\tau}\tau\right)\frac{d\lambda}{d\tau} - \left(a_2\lambda e^{-\lambda\tau} + a_4 e^{-\lambda\tau}\right)\lambda = 0. \tag{19}$$

Thus,

$$\left(\frac{d\lambda}{d\tau}\right)^{-1} = \frac{2\lambda + a_1 + a_2 e^{-\lambda\tau}}{(a_2\lambda + a_4)\lambda e^{-\lambda\tau}} - \frac{\tau}{\lambda}. \tag{20}$$

From equation (10), we get

$$e^{-\lambda\tau} = \frac{-\lambda^2 - a_1\lambda - a_3}{a_2\lambda + a_4}.$$

Using the above fact,

$$\left[\left(\frac{d\lambda}{d\tau}\right)^{-1}\right]_{\tau=\tau_j^{\pm}} = \left[\frac{-2\lambda - a_1}{\lambda(\lambda^2 + a_1\lambda + a_3)} + \frac{a_2}{\lambda(a_2\lambda + a_4)} - \frac{\tau}{\lambda}\right]_{\lambda=i\omega_{\pm}}$$

$$= \frac{a_1^2 - 2(a_3 - \omega^2)}{a_1^2\omega^2 + (\omega^2 - a_3)^2} - \frac{a_2^2}{a_2^2\omega^2 + a_4^2} + \operatorname{Im}\left[\left(\frac{d\lambda}{d\tau}\right)^{-1}\right]_{\tau=\tau_j^{\pm}}.$$

Now, we observe that

$$\operatorname{sign}\left\{\left[\frac{d(\operatorname{Re}\lambda)}{d\tau}\right]_{\tau=\tau_j^{\pm}}\right\} = \operatorname{sign}\left\{\operatorname{Re}\left[\left(\frac{d\lambda}{d\tau}\right)^{-1}\right]_{\tau=\tau_j^{\pm}}\right\}$$

$$= \operatorname{sign}\left\{\frac{a_1^2 - 2(a_3 - \omega^2)}{a_1^2\omega^2 + (\omega^2 - a_3)^2} - \frac{a_2^2}{a_2^2\omega^2 + a_4^2}\right\}$$

$$= \operatorname{sign}\{a_1^2 - a_2^2 - 2a_3 + 2\omega^2\}$$

$$\left[\text{as } a_1^2\omega^2 + (\omega^2 - a_3)^2 = a_2^2\omega^2 + a_4^2 \text{ by Equation (14)}\right]$$

$$= \operatorname{sign}\left\{\pm\sqrt{\Delta}\right\},$$

where $\Delta = (a_2^2 - a_1^2 + 2a_3)^2 - 4(a_3^2 - a_4^2)$.

Hence, we obtain the transversality conditions

$$\left[\frac{d(\operatorname{Re}\lambda)}{d\tau}\right]_{\tau=\tau_j^+} > 0 \quad \text{and} \quad \left[\frac{d(\operatorname{Re}\lambda)}{d\tau}\right]_{\tau=\tau_j^-} < 0, \text{ provided } \Delta \neq 0.$$

Remark 4.2. It is noted that in **Case 3**, we have found a twofold ω, and hence, $\Delta = 0$. Consequently, $\operatorname{sign}\left\{\pm\sqrt{\Delta}\right\} = 0$, and we conclude that no crossing of eigenvalues from $\mathbb{C}^-$ plane to $\mathbb{C}^+$ plane (or vice-versa) takes place.

Further, from the conditions obtained in **Cases 2** and **4**, it is observed that the purely imaginary roots $\omega_{\pm}$ of the characteristic equation (10) are simple. As a result, a pair of eigenvalues enters into the right-half complex plane $\mathbb{C}^+$ (resp. left-half complex plane $\mathbb{C}^-$) when τ increases through τ_j^+ (resp. τ_j^-). When $\tau = \{\tau_j^{\pm}\}$, $j = 0, 1, 2, \ldots$, the following result holds true:

Result 4.3. *Hopf-bifurcation in the system occurs at each value of time delay* $\tau = \{\tau_j^{\pm}\}$, *where* $j = 0, 1, 2, \ldots$

We state the following Lemma due to Cooke and Grossman[40] to understand the change in number of eigenvalues when τ varies.

Lemma 4.1 (Cooke and Grossman[40]). *Let* $f(\lambda, \tau) = \lambda^2 + d_1\lambda + d_2\lambda e^{-\lambda\tau} + d_3 + d_4 e^{-\lambda\tau}$, *where* $d_i's$ $(i = 1, 2, 3, 4)$ *and* τ *are real numbers and* $\tau > 0$. *Then, as* τ *varies, the sum of the multiplicities of zeros of* f *in the open right half-plane can change only if a zero appears on or crosses the imaginary axis.*

It is to be noted that conditions of **Case 1** are the necessary as well as sufficient for the system to undergo no change in its stability (resp. instability) nature. Further, the conditions in **Case 2** (resp. **Case 3**) are necessary for change of stability (resp. stability switching). Thus, based on the above discussions, the following theorems are presented to understand the stability phenomenon of the two interior equilibria.

Theorem 4.2. *If either* $(a_2^2 - a_1^2 + 2a_3) < 0$ *and* $(a_3^2 - a_4^2) > 0$ *or* $(a_2^2 - a_1^2 + 2a_3)^2 < 4(a_3^2 - a_4^2)$ *following **Case 1** are satisfied, then there does not exist any critical time delays. Thus, the stability (resp. instability) of any interior equilibrium* $E = (x^*, y^*)$ *remains unchanged for* $\tau > 0$.

Theorem 4.3. *If an interior equilibrium $E = (x^*, y^*)$ is stable in absence of τ, and the condition $a_3^2 - a_4^2 < 0$ following* **Case 2** *is satisfied, then stability of the interior equilibrium changes.*

Theorem 4.4. *If an interior equilibrium $E = (x^*, y^*)$ is stable in absence of τ, and the conditions $a_3^2 - a_4^2 > 0$, $a_2^2 - a_1^2 + 2a_3 > 0$, and $(a_2^2 - a_1^2 + 2a_3)^2 > 4(a_3^2 - a_4^2)$ in* **Case 4** *are satisfied, then the following cases hold:*

1. *A change in the stability takes place whenever $0 < \tau_0^+ < \tau_1^+ < \tau_0^-$.*
2. *A finite k number of stability switching occurs whenever $0 < \tau_0^+ < \tau_0^- < \tau_1^+ < \tau_1^- < \cdots < \tau_k^+ < \tau_{k+1}^+ < \tau_k^- < \ldots$. Eventually for $\tau > \tau_k^+$, the equilibrium remains unstable.*

Theorem 4.5. *If an interior equilibrium $E = (x^*, y^*)$ is unstable in absence of τ, and the condition $a_3^2 - a_4^2 < 0$ in* **Case 2** *is satisfied, then the existence of τ_j^+ ($j = 0, 1, 2, \ldots$) corresponding to the positive ω_+ cannot lead to change in its instability.*

Theorem 4.6. *If an interior equilibrium $E = (x^*, y^*)$ is unstable in absence of τ, and the conditions $a_3^2 - a_4^2 > 0$, $a_2^2 - a_1^2 + 2a_3 > 0$, and $(a_2^2 - a_1^2 + 2a_3)^2 > 4(a_3^2 - a_4^2)$ in* **Case 4** *are satisfied, then the following cases hold:*

1. *the system remains unstable for all τ whenever $0 < \tau_0^+ < \tau_1^+ < \tau_0^-$.*
2. *a finite k number of instability switching occurs whenever $0 < \tau_0^- < \tau_0^+ < \tau_1^- < \tau_1^+ < \cdots < \tau_k^+ < \tau_{k+1}^+ < \tau_k^- < \ldots$. Finally for $\tau > \tau_k^+$, the equilibrium retains its instability.*

Proof.

(1.) Initially there exist a pair of roots in $\mathbb{C}^+$ when $\tau = 0$. As the conditions in **Case 4** are satisfied, this leads to existence of $\omega_\pm$. The corresponding values of critical time delays are given from expression (18). As mentioned in Lemma 4.1, the sum of multiplicities of roots in $\mathbb{C}^+$ will change only when a root appears on or crosses the imaginary axis. So in addition to the pair of roots that are already in $\mathbb{C}^+$ at $\tau = 0$, multiplicity of the roots in $\mathbb{C}^+$ increased by 2 immediately after τ is increased and passes through τ_0^+. Next, when τ passes through τ_1^+, another pair of roots is added in $\mathbb{C}^+$. Now, further increase in τ through τ_0^- cannot change the instability since a pair of roots still persist in $\mathbb{C}^+$. However, three consecutive appearance of τ_0^-, τ_1^-, and τ_2^- in between τ_1^+ and τ_2^+ can change the instability. But from equation (15), we have $\omega_+ > \omega_-$. So, from expression (18), we get $|\tau_{i+1}^+ - \tau_i^+| = \frac{2\pi}{\omega_+} < \frac{2\pi}{\omega_-} = |\tau_{i+1}^- - \tau_i^-|$. Henceforth, two consecutive τ_0^- and τ_1^- is impossible to appear in between τ_1^+ and τ_2^+ since the distance between two τ_i^+ are always less than the distance between two consecutive τ_i^-, ($i = 1, 2, 3, \ldots$). Thus, instability persevere for all τ.

(2.) In absence of delay, there exist a pair of roots in $\mathbb{C}^+$. Once τ reaches τ_0^-, a pair of imaginary roots lie on $\mathbb{C}^0$. Then, with increase in the value of τ through τ_0^-, multiplicity of roots in $\mathbb{C}^+$ decreases by two. Henceforth, the equilibrium becomes stable. Again with increase in τ through τ_0^+, multiplicity of roots in $\mathbb{C}^+$ will increase by 2. Thus, the system becomes unstable again. Using the same arguments as above, instability switching will continue until the appearance of two consecutive τ_{k+1}^+ and τ_k^+ together, beyond which instability persists.

$\square$

Theorem 4.7. *If an interior equilibrium $E = (x^*, y^*)$ is a saddle point when $\tau = 0$, then the equilibrium cannot be stable for varying delay τ.*

Proof. Since the interior equilibrium $E = (x^*, y^*)$ is a saddle point, one of the two eigenvalues of the characteristic function (11) must lie in $\mathbb{C}^+$ plane and the other eigenvalue lies in $\mathbb{C}^-$ plane. The equilibrium becomes stable for some τ only when no eigenvalues lie in the $\mathbb{C}^+$ plane. Now, as mentioned in Lemma 4.1,[40] with increase in τ, the sum of multiplicities of zeros of the characteristic equation (10) in the $\mathbb{C}^+$ plane can change only if a zero appears on or cross imaginary axis. This means that, without this process, no eigenvalues are immersed in $\mathbb{C}^+$ plane. But the crossing of eigenvalues occurs in pair. Since only a single eigenvalue lies in $\mathbb{C}^+$ plane, it can never cross the $\mathbb{C}^0$ axis. Thus the system cannot become stable for any $\tau > 0$. $\square$

Analytical prove is provided for Theorems 4.6 and 4.7. However, the theorems (Theorems 4.2–4.6) are not validated yet. Several articles presented mathematical conditions for the (non) existence of positive ω to depict the delay induced

dynamics. However, some contributions did not prove the validity of the mathematical conditions in a general parameter space.[14,31] Morever, the mathematical conditions are not verified numerically. We now recall **Cases 1** to **4** for the (non) existence of ω. We examine whether these cases could be possible under certain parameter sets. The illustrations in the succeeding sections reflect a more clear-cut depiction of the stability behavior of system (4) under mathematical conditions mentioned in **Cases 1, 2** and **4**, and verify Theorems 4.2–4.7 with respect to our system (4).

4.1 | No change in stability

The below example satisfies Theorems 4.2, 4.5, and 4.7.

Example 4.1. We consider the parameter values for system (4) as $r = 0.5$, $K = 400$, $\alpha = 0.03$, $\beta = 0.01$, $\gamma = 0.01$, $m = 0.1$, and $C = 50$. The trivial equilibrium $(0, 0)$ and boundary equilibrium $(400, 0)$ always exist, and their stability behavior is shown analytically. We focus to investigate the stability of the coexisting equilibria in all the examples. The two interior equilibria are $E_1 = (113.8600, 11.9225)$ and $E_2 = (359.7400, 1.6775)$. We find $a_1 + a_2 = 0.0702 > 0$ and $a_3 + a_4 = 0.0845 > 0$ at the interior equilibrium E_1. Thus, E_1 is locally stable when $\tau = 0$. Now, $(a_2^2 - a_1^2 + 2a_3)^2 - 4(a_3^2 - a_4^2) = -0.0068 < 0$ at E_1, i.e., the condition in **Case 1** is satisfied at E_1. Hence no real ω exists. Thus, the equilibrium E_1 remains locally stable for all time delays.

On the other hand, $a_1 + a_2 = 0.3535 > 0$ and $a_3 + a_4 = -0.0374 < 0$ at the interior equilibrium E_2, which indicate that E_2 is a saddle point (unstable) when $\tau = 0$. Hence, by Theorem 4.7, we obtain no change in stability due to varying delay. Alternatively, we can explore how the internal mechanism works to maintain its instability. We note that $a_3^2 - a_4^2 = -0.0059 < 0$ associated with E_2. Thus, a positive $\omega_+ = 0.1728$ exists by **Case 2**. The corresponding $\tau_0^+ = 31.1886$ has the transversality condition $\left[\frac{d(\text{Re}\lambda)}{d\tau}\right]_{\tau=\tau_0^+} > 0$. Therefore, a pair of eigenvalues with negative real parts shift from $\mathbb{C}^-$ plane to $\mathbb{C}^+$ plane. Thus, no change in the instability is observed. Henceforth, numerically too, we conclude that E_2 undergoes no change in its instability. The same result is stated in Theorem 4.5. We further plot some of the real parts of the roots of the characteristic function associated with E_2, to examine how they evolve with delay (Figure 1). It is clear from Figure 1 that a positive root always exists independent of the values of time delays. However, a pair of eigenvalues crosses $\mathbb{C}^0$ at $\tau_0^+ = 31.1886$ since the transversality condition $\left[\frac{d(\text{Re}\lambda)}{d\tau}\right]_{\tau=\tau_0^+} > 0$ is satisfied. Note that many eigenvalues with negative real parts are originated when τ increases. The presence of positive real parts of the roots indicates the instability which persists for E_2 for all time delay.

Generally, local dynamics around a stable (an unstable) equilibrium changes its stability in delayed population models once the first critical threshold exists. To the best of the knowledge, the scenario is different for the saddle
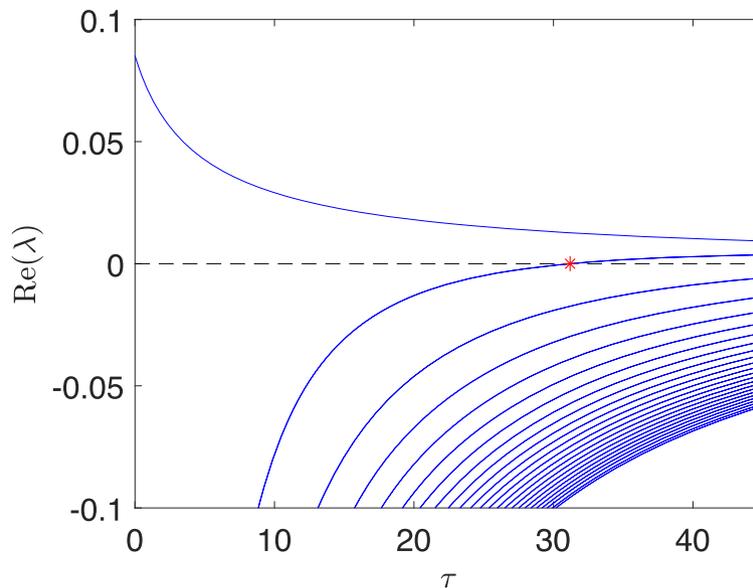
FIGURE 1 The real part of the roots of the characteristic function are plotted for varying τ corresponding to $E_2 = (359.7400, 1.6775)$ for the set of parameter values $r = 0.5$, $K = 400$, $\alpha = 0.03$, $\beta = 0.01$, $\gamma = 0.01$, $m = 0.1$, and $C = 50$. A pair of eigenvalues crosses $\mathbb{C}^0$ at $\tau_0^+ = 31.1886$ (indicated in red star) [Colour figure can be viewed at wileyonlinelibrary.com]

(A)

(B)

(C)

(D)
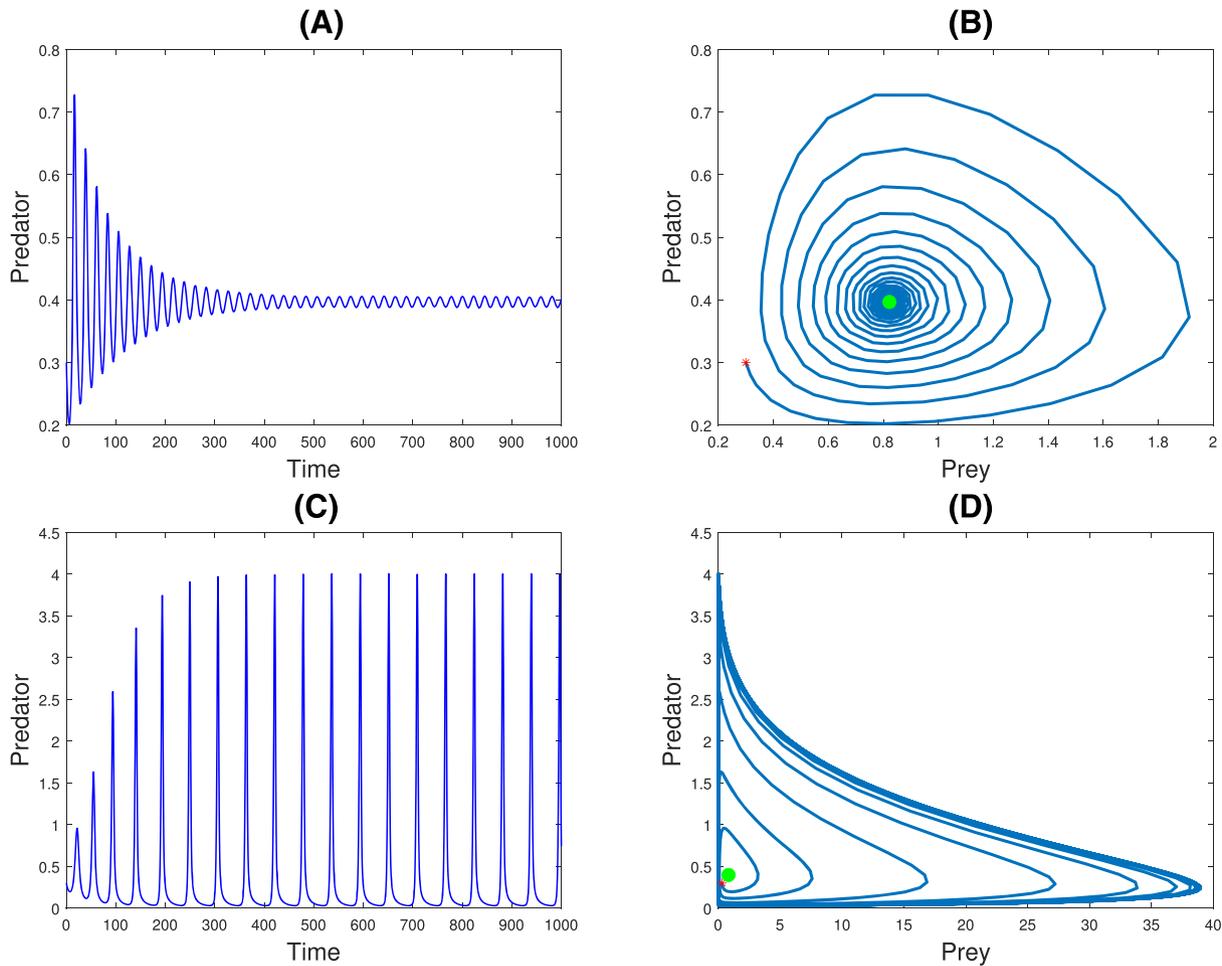
FIGURE 2 The time series evolution of the predator for the parameters $r = 0.4$, $K = 100$, $\alpha = 1$, $\beta = 0.9$, $\gamma = 0.8$, $m = 0.01$, and $C = 0.5$ with the initial conditions $(0.3, 0.3)$, is plotted in (A) when $\tau = 1$ and in (C) when $\tau = 3$. The corresponding phrase portraits with the same initial conditions (indicated in red) are shown in (B) when $\tau = 1$ and in (D) when $\tau = 3$. The equilibrium $E_1 = (0.8222, 0.3967)$ (indicated in green) is locally stable when $\tau = 1$ and is unstable when $\tau = 3$ as shown in (A) and (D), respectively [Colour figure can be viewed at wileyonlinelibrary.com]

equilibrium in our model which has not been explored before. Overall, it can be concluded in this example that E_1 is locally stable and E_2 is saddle for all time delay. Also, we proved analytically that the stability of the trivial equilibrium and the boundary equilibrium do not depend on delay. So the system experiences no change in dynamics due to varying τ.

4.2 | Stability change

In the following example, Theorems 4.3 and 4.7 are validated for our system (4).

Example 4.2. If the parameters for system (4) are: $r = 0.4$, $K = 100$, $\alpha = 1$, $\beta = 0.9$, $\gamma = 0.8$, $m = 0.01$, and $C = 0.5$, then the two interior equilibria $E_1 = (0.8222, 0.3967)$ and $E_2 = (99.9860, 0.000055)$ come into existence. Here, $a_1 + a_2 = 0.1303 > 0$ and $a_3 + a_4 = 0.1381 > 0$ at the equilibrium E_1. Hence E_1 is stable when $\tau = 0$. The condition of **Case 2** is satisfied at E_1, i.e., $a_3^2 - a_4^2 = -0.0164 < 0$. Consequently, one positive $\omega_+ = 0.2685$ is acquired. The first critical time delay is $\tau_0^+ = 1.3779$, and the transversality condition $\left[\frac{d(\text{Re}\lambda)}{d\tau} \right]_{\tau=\tau_0^+} > 0$ is satisfied at τ_0^+. The equilibrium E_1 is stable (Figure 2A, B) when $\tau < \tau_0^+$. If $\tau = \tau_0^+$, a Hopf-bifurcation occurs at E_1. Further increasing the value of $\tau (> \tau_0^+)$, a pair of eigenvalues cross $\mathbb{C}^0$ from $\mathbb{C}^-$ to $\mathbb{C}^+$. Hence, E_1 becomes unstable (Figure 2C, D). Since the transversality condition $\left[\frac{d(\text{Re}\lambda)}{d\tau} \right]_{\tau=\tau_j^+} > 0$ holds at every critical threshold of delay, on any interval (τ_j^+, τ_{j+1}^+)
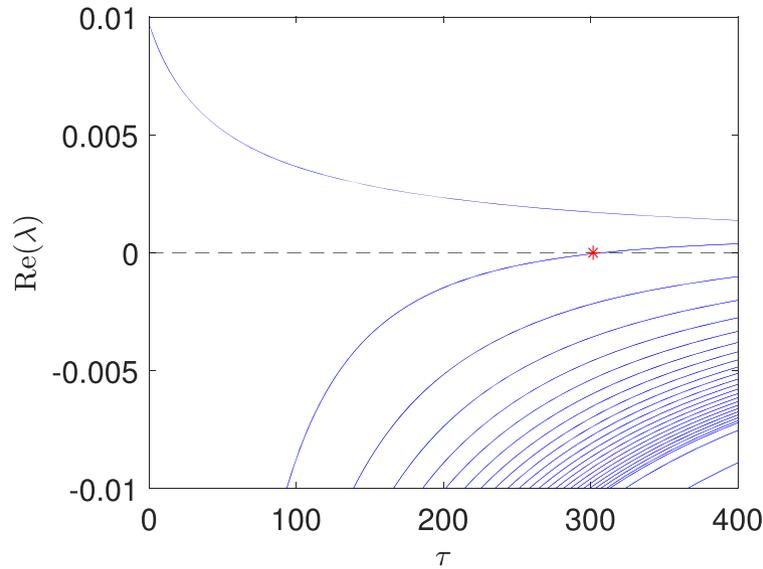
FIGURE 3 The real part of the eigenvalues of the characteristic function are plotted with respect to varying τ. Here, the red star represents the eigenvalue with zero real part corresponding to the critical $\tau_0^+ = 301.6067$. It can be seen that positive real parts of the eigenvalues exist for all time delays considered, which maintains the instability of the corresponding equilibrium. The parameter set are $r = 0.4$, $K = 100$, $\alpha = 1$, $\beta = 0.9$, $\gamma = 0.8$, $m = 0.01$, $C = 0.5$, and the equilibrium is $E_2 = (99.9860, 0.000055)$ [Colour figure can be viewed at wileyonlinelibrary.com]

TABLE 1 Some of the values of $\tau_j^{\pm}$ ($j = 0, 1, 2, 3, 4, 5$) for the same parameter set corresponding to Example 4.3

τ_j^+	$\tau_0^+ \approx 6.2959$	$\tau_1^+ \approx 41.0120$	$\tau_2^+ \approx 75.7281$	$\tau_3^+ \approx 110.4442$	$\tau_4^+ \approx 145.1603$	$\tau_5^+ = 179.8764$
τ_j^-	$\tau_0^- \approx 51.8174$	$\tau_1^- \approx 181.7683$	$\tau_2^- \approx 311.7192$	$\tau_3^- \approx 441.6701$	$\tau_4^- \approx 571.6210$	$\tau_5^- \approx 701.5719$

($j = 1, 2, \ldots$), the number of eigenvalues with positive real parts is $2j$. Therefore, E_1 remains unstable for all $\tau > \tau_0^+$ as stated in Theorem 4.3. Now, corresponding to the equilibrium E_2, $a_1 + a_2 = 0.3899 > 0$ and $a_3 + a_4 = -0.0040 < 0$. This confirms that E_2 is a saddle point when $\tau = 0$. Hence, E_2 will remain saddle for varying delay τ, as stated in Theorem 4.7. We can also address this result numerically. For E_2, we have $a_3^2 - a_4^2 = -0.00004825$. Consequently, one positive $\omega_+ = 0.0174$ exists as discussed in **Case 2**. Corresponding to threshold $\tau_0^+ = 301.6$, the transversality condition $\left[\frac{d(\text{Re}\lambda)}{d\tau}\right]_{\tau=\tau_0^+} > 0$ is satisfied. Thus, E_2 remains saddle for all time delay. In Figure 3, real parts of some of the roots of the characteristic function are plotted for varying time delay to visualize the nature of stability of the equilibrium E_2.

Next, we provide an example to understand the validity of the Theorem 4.4 in our system (4).

Example 4.3. The parameters $r = 0.8$, $K = 45$, $\alpha = 0.07$, $\beta = 0.04$, $\gamma = 0.001$, $m = 0.3$, and $C = 5.6888$ generate two interior equilibria $E_1 = (13.1132, 8.0982)$ and $E_2 = (39.7646, 1.3296)$. Here, E_1 is stable for $\tau = 0$ since $a_1 + a_2 = 0.1141 > 0$ and $a_3 + a_4 = 0.14690.1469 > 0$ at E_1. The conditions of **Case 4** are satisfied at E_1, i.e., $a_3^2 - a_4^2 = 0.00007 > 0$, $a_2^2 - a_1^2 + 2a_3 = 0.0351 > 0$, and $(a_2^2 - a_1^2 + 2a_3)^2 - 4(a_3^2 - a_4^2) = 0.0009 > 0$. Therefore, $\omega_+ = 0.1810$ and $\omega_- = 0.0484$ are obtained. The numerical values of the critical time delays are supplied in Table 1. The distribution of the critical time delays in ascending order based on their numerical values are as follows:

$$\tau_0^+ < \tau_1^+ < \tau_0^- < \tau_2^+ < \tau_3^+ < \tau_4^+ < \tau_5^+ < \tau_1^- < \ldots .$$

Based on the distribution of the critical delays, it is observed that the conditions of Theorem 4.4 hold true, and hence, E_1 changes its stability. The time series for some values of τ are provided in Figure 4A–C, which clearly illustrates the stability changing nature of E_1. The real parts of eigenvalues for the characteristic function associated with E_1 is plotted in Figure 4D to support our obtained results. For the equilibrium E_2, we find that $a_1 + a_2 = 0.4640 > 0$ and $a_3 + a_4 = -0.1437 < 0$ which confirm that E_2 is a saddle point in absence of time delay. Hence by Theorem 4.7, we conclude that E_2 remains saddle for varying time delay.
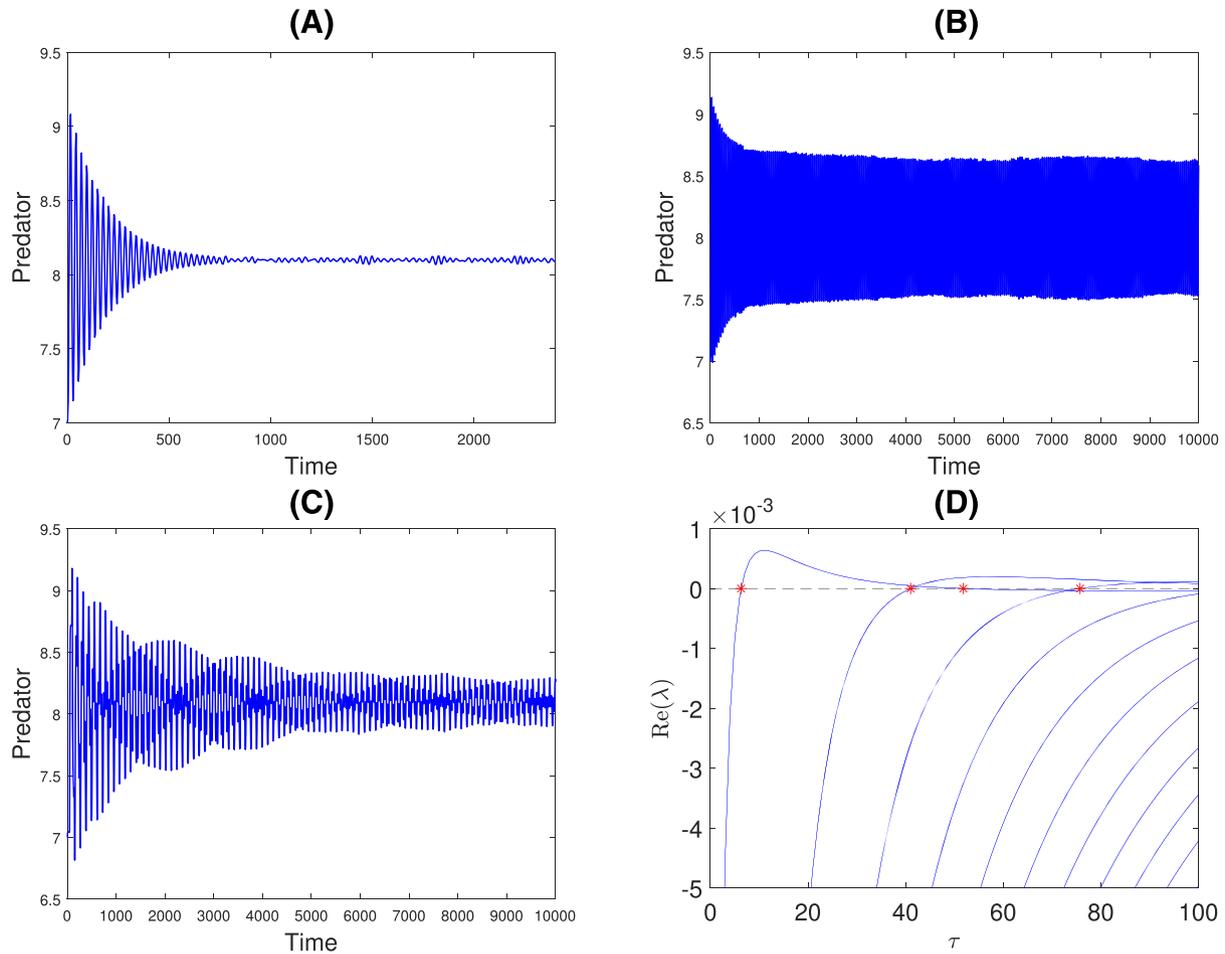
FIGURE 4 For the initial conditions $(14, 7)$, the solution is plotted for (A) $\tau = 3$, (B) $\tau = 9$, and (C) $\tau = 45$ with the parameters $r = 0.8$, $K = 45$, $\alpha = 0.07$, $\beta = 0.04$, $\gamma = 0.001$, $m = 0.3$, and $C = 5.6888$. The equilibrium $(13.1132, 8.0982)$ is stable for $\tau < 6.2959$ and unstable for all $\tau > 6.2959$. (D) The real parts of the eigenvalues are plotted for varying τ. The red stars represent the critical delays $\tau_0^+ = 6.2959$, $\tau_1^+ = 41.0120$, $\tau_0^- = 51.8174$, and $\tau_2^+ = 75.7281$ [Colour figure can be viewed at wileyonlinelibrary.com]

TABLE 2 Some of the values of $\tau_j^\pm$ ($j = 0, 1, 2, 3$) for parameters $r = 0.5$, $K = 400$, $\alpha = 0.03$, $\beta = 0.01$, $\gamma = 0.01$, $m = 0.1$, and $C = 39.6$

τ_j^+	$\tau_0^+ \approx 9.0221$	$\tau_1^+ \approx 59.9663$	$\tau_2^+ \approx 110.9105$	$\tau_3^+ \approx 161.8547$
τ_j^-	$\tau_0^- \approx 26.4507$	$\tau_1^- \approx 117.6972$	$\tau_2^- \approx 208.9436$	

4.3 | Stability switching

In the following two examples, Theorem 4.4 is satisfied.

Example 4.4. The parameters $r = 0.5$, $K = 400$, $\alpha = 0.03$, $\beta = 0.01$, $\gamma = 0.01$, $m = 0.1$, and $C = 39.6$ produce two interior equilibria $E_1 = (93.3713, 12.7762)$ and $E_2 = (370.2447, 1.2398)$. The equilibrium E_1 is a stable focus due to existence of eigenvalues $-0.0361362 \pm 0.284262i$ when $\tau = 0$. The conditions of **Case 4**, i.e., $a_3^2 - a_4^2 = 0.00007212 > 0$, $a_2^2 - a_1^2 + 2a_3 = 0.0200 > 0$, and $(a_2^2 - a_1^2 + 2a_3)^2 - 4(a_3^2 - a_4^2) = 0.0001096 > 0$, are satisfied corresponding to E_1. Hence, two positive ω, viz., $\omega_+ = 0.1233$ and $\omega_- = 0.0689$ exist. The values of the critical time delays are supplied in Table 2, and they are arranged in ascending orders as

$$\tau_0^+ < \tau_0^- < \tau_1^+ < \tau_2^+ < \tau_2^- < \tau_3^+ < \dots.$$

It can be concluded that E_1 remains stable till $\tau < \tau_0^+$. When $\tau = \tau_0^+$, the transversality condition $\left[\frac{d(\mathrm{Re}\lambda)}{d\tau}\right]_{\tau = \tau_0^+} > 0$ is satisfied which indicates that a pair of eigenvalues with negative real parts shifts to the right half plane C^+. Thus, once
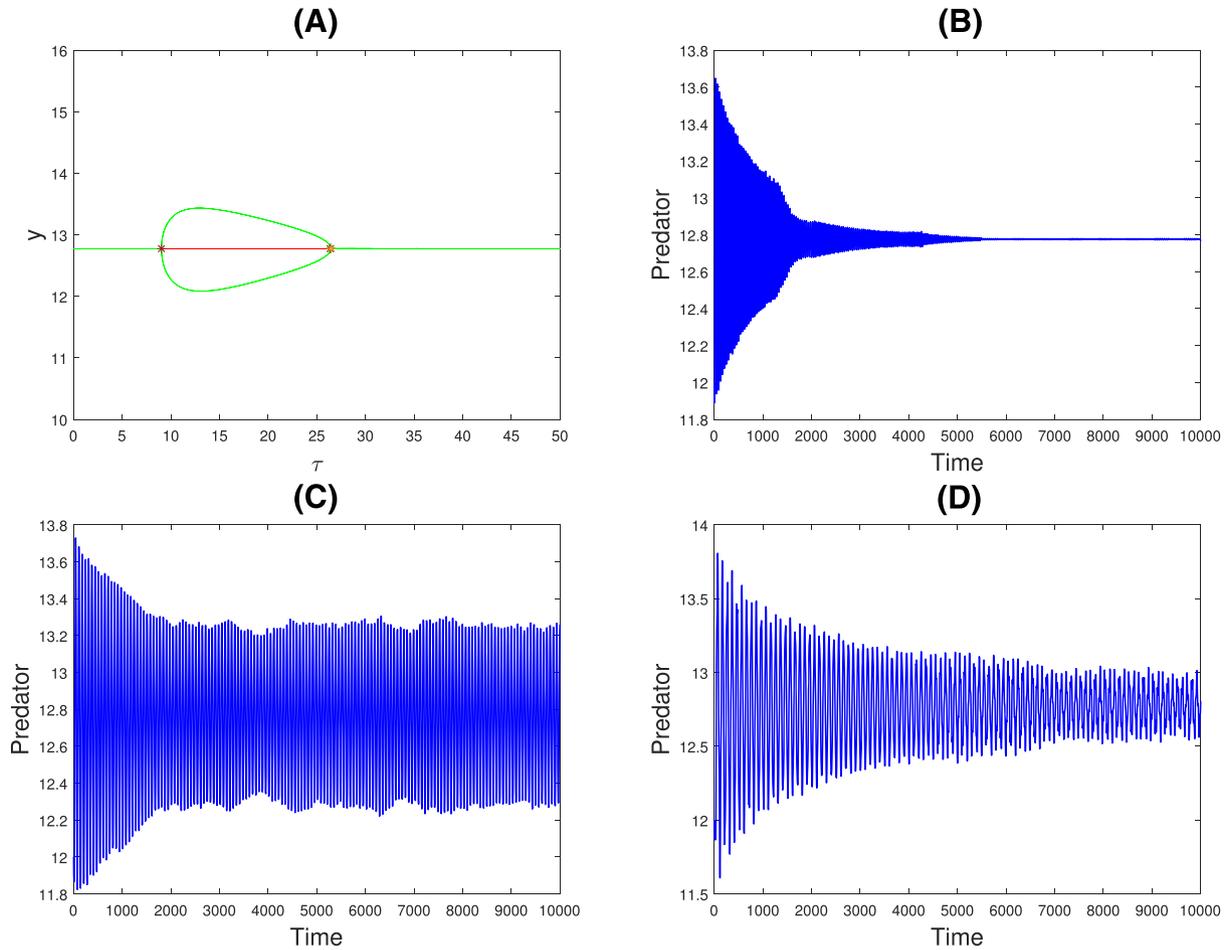
FIGURE 5 (A) The bifurcation diagram with respect to predator population when τ is varied. The predator response in time corresponding to the equilibrium E_1 is plotted for (B) $\tau = 5$, (C) $\tau = 15$, and (D) $\tau = 30$. The parameter values provided are $r = 0.5$, $K = 400$, $\alpha = 0.03$, $\beta = 0.01$, $m = 0.1$, $\gamma = 0.01$, and $C = 39.6$ with the initial conditions (93,12) [Colour figure can be viewed at wileyonlinelibrary.com]

$\tau > \tau_0^+$, E_1 becomes unstable due to the presence of eigenvalues with positive real parts. Again, when the next critical value τ_0^- is obtained, a pair of positive eigenvalues shifts from C^+ to the left half plane C^- since the transversality condition $\left[\frac{d(\text{Re}\lambda)}{d\tau}\right]_{\tau=\tau_0^-} < 0$ holds. This makes the equilibrium E_1 stable again. With further increase in τ, it is noticed from Table 2 that the succeeding critical delays after τ_0^- are τ_1^+ and τ_2^+. Thus, eigenvalues with positive real parts always exist for the characteristic equation (10) whenever $\tau > \tau_1^+$. This suggests that the system remains unstable once the time delay becomes grater than τ_1^+. The stability switching naure at E_1 is illustrated in Figure 5 by choosing some values of time delay.

Now, the other interior equilibrium E_2 is a saddle point (unstable) when $\tau = 0$ due to existence of a positive root 0.0890 and a negative root -0.4552 of the characteristic function. The conditions mentioned above are met, i.e., $a_3^2 - a_4^2 = -0.0063 < 0$. So a positive $\omega_+ = 0.1732$ exists. However, for the critical time delay $\tau_0^+ = 6.4243$, the transversality condition $\left[\frac{d(\text{Re}\lambda)}{d\tau}\right]_{\tau=\tau_j^+} > 0$ holds. Henceforth, E_2 remains unstable for all time delay.

We provide another example to explain that multiple stability switching may take place in the system.

Example 4.5. We choose the parameters as $r = 0.4$, $K = 100$, $\alpha = 1$, $\beta = 0.9$, $\gamma = 0.8$, $m = 0.1$, and $C = 20$ and obtain the interior equilibria $E_1 = (25.6227, 0.2975)$ and $E_2 = (92.5570, 0.0297)$. Corresponding to E_1, $a_1 + a_2 = 0.0074$ and $a_3 + a_4 = 0.0908$, which confirm the stability of E_1 in absence of τ. Further, we determine $a_3^2 - a_4^2 = 0.0025$, $a_2^2 - a_1^2 + 2a_3 = 0.1080$, and $(a_2^2 - a_1^2 + 2a_3)^2 - 4(a_3^2 - a_4^2) = 0.0018$, and corresponding $\omega_+ = 0.2739$ and $\omega_- = 0.1816$. The numerical values of the critical delays are provided in Table 3. The distribution of the critical delays in ascending

order are as follows:

$$\tau_0^+ < \tau_0^- < \tau_1^+ < \tau_1^- < \tau_2^+ < \tau_3^+ < \tau_2^- < \tau_4^+ < \tau_3^- < \tau_5^+ < \ldots \, .$$

Based on this distribution of the critical values, we can infer that, when the critical delays are in the range $(0, \tau_0^+)$, the equilibrium E_1 is stable. A Hopf-bifurcation occurs at $\tau = \tau_0^+$. Further increase in the values of delay leads to instability till the threshold $\tau = \tau_0^-$. For $\tau = \tau_0^-$, a Hopf-bifurcation occurs. Again, when τ lies in the range (τ_0^-, τ_1^+), stability is regained for E_1. This switching of stability repeats till $\tau = \tau_2^+$. When $\tau = \tau_2^+$, another Hopf-bifurcaton occurs, and further increase of τ leads to instability forever.

The bifurcation diagram with respect to the predator population, when the critical delays are varied, is supplied in Figure 6. It can be seen in the figure that the two bubbles appear which represent the two stability switching.

On the other hand, at E_2, we have $a_1 + a_2 = 0.2704$ and $a_3 + a_4 = -0.0333$, which indicate that E_2 is a saddle point when $\tau = 0$. Hence, by Theorem 4.7, we conclude that no change in the stability occurs at E_2.

4.4 | No change in instability

The below example satisfies Theorems 4.6 and 4.7.

Example 4.6. We take the parameter set as $r = 0.34$, $K = 102$, $\alpha = 1$, $\beta = 0.9$, $\gamma = 0.8$, $m = 0.1$, and $C = 16.9$. Two interior equilibria are $E_1 = (22.4506, 0.2652)$ and $E_2 = (94.9394, 0.0235)$. The equilibrium E_1 is unstable focus in the absence of τ, since $a_1 + a_2 = -0.0203 < 0$ and $a_3 + a_4 = 0.0756 > 0$. At E_1, $a_3^2 - a_4^2 = 0.00021$, $a_2^2 - a_1^2 + 2a_3 = 0.1033$, and $(a_2^2 - a_1^2 + 2a_3)^2 - 4(a_3^2 - a_4^2) = 0.0098$. Thus, the conditions mentioned in **Case 4** are met here. These conditions lead to $\omega_+ = 0.3180$ and $\omega_- = 0.0460$. The values of critical time delays are supplied in Table 4. However, it can be seen from the table, that the appearance of two consecutive τ_0^+ and τ_1^+ never makes the equilibrium E_1 stable. Hence, instability persists for all time delay around E_1.

Now, for the equilibrium E_2, we have $a_1 + a_2 = 0.2166$ and $a_3 + a_4 = -0.0288$, which indicate E_2 to be a saddle point when $\tau = 0$. As quoted in Theorem 4.7, the equilibrium E_2 could not alter its stability.

TABLE 3 Some of the values of $\tau_j^\pm$ ($j = 0, 1, 2, 3$) for parameter sets $r = 0.4$, $K = 100$, $\alpha = 1$, $\beta = 0.9$, $\gamma = 0.8$, $m = 0.1$, and $C = 20$

τ_j^+	$\tau_0^+ \approx 0.3114$	$\tau_1^+ \approx 23.2482$	$\tau_2^+ \approx 46.1851$	$\tau_3^+ \approx 69.1219$	$\tau_4^+ = 92.0587$	$\tau_5^+ = 114.9956$
τ_j^-	$\tau_0^- \approx 2.5518$	$\tau_1^- \approx 37.1476$	$\tau_2^- \approx 71.7435$	$\tau_3^- \approx 106.3394$	$\tau_4^- = 140.9353$	$\tau_5^- = 175.5312$
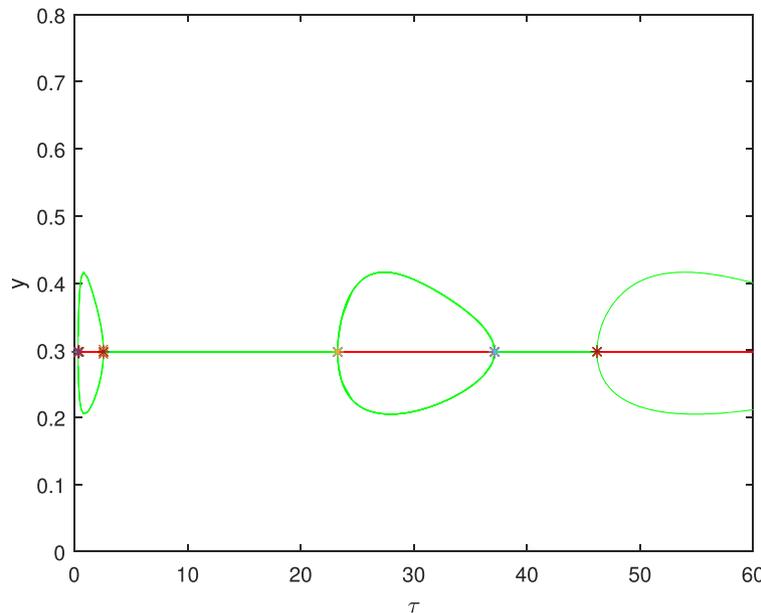
FIGURE 6 The bifurcation diagram in terms of predator population under varying τ for the parameter values $r = 0.4$, $K = 100$, $\alpha = 1$, $\beta = 0.9$, $\gamma = 0.8$, $m = 0.1$, and $C = 20$ [Colour figure can be viewed at wileyonlinelibrary.com]

TABLE 4 Some of the values of $\tau_j^\pm$ ($j = 0, 1, 2, 3$) for the parameter set $r = 0.34$, $K = 102$, $\alpha = 1$, $\beta = 0.9$, $\gamma = 0.8$, $m = 0.1$, and $C = 16.9$

τ_j^+	$\tau_0^+ \approx 19.3433$	$\tau_1^+ \approx 39.0997$	$\tau_2^+ \approx 58.8562$	$\tau_3^+ \approx 78.6127$
τ_j^-	$\tau_0^- \approx 40.0435$	$\tau_1^- \approx 176.7829$	$\tau_2^- \approx 313.5223$	$\tau_3^- \approx 450.2618$

TABLE 5 Some of the values of $\tau_j^\pm$ ($j = 0, 1, 2, 3, 4, 5$) for the parameter set $r = 0.4$, $K = 100$, $\alpha = 1$, $\beta = 0.9$, $\gamma = 0.8$, $m = 0.1$, and $C = 16.9$

τ_j^+	$\tau_0^+ \approx 18.4872$	$\tau_1^+ \approx 37.1166$	$\tau_2^+ \approx 55.7459$	$\tau_3^+ \approx 74.3753$	$\tau_4^+ \approx 93.0047$	$\tau_5^+ \approx 111.6340$
τ_j^-	$\tau_0^- \approx 105.5391$	$\tau_1^- \approx 369.1680$	$\tau_2^- \approx 632.7968$	$\tau_3^- \approx 896.4256$	$\tau_4^- \approx 1160.0544$	$\tau_5^- \approx 1423.6832$

TABLE 6 Some of the values of $\tau_j^\pm$ ($j = 0, 1, 2, 3, 4$) when $r = 1.2$, $K = 80$, $\alpha = 0.2$, $\beta = 0.1$, $m = 2.0$, $C = 2.1$, and $\gamma = 0.001$

τ_j^+	$\tau_0^- \approx 1.0035$	$\tau_1^- \approx 12.4723$	$\tau_2^- \approx 23.9411$	$\tau_3^- \approx 35.4099$	$\tau_4^- \approx 46.8787$	$\tau_5^- \approx 58.3475$
τ_j^-	$\tau_0^+ \approx 3.4262$	$\tau_1^+ \approx 7.0883$	$\tau_2^+ \approx 10.7503$	$\tau_3^+ \approx 14.4124$	$\tau_4^+ \approx 18.0744$	$\tau_5^+ \approx 21.7364$
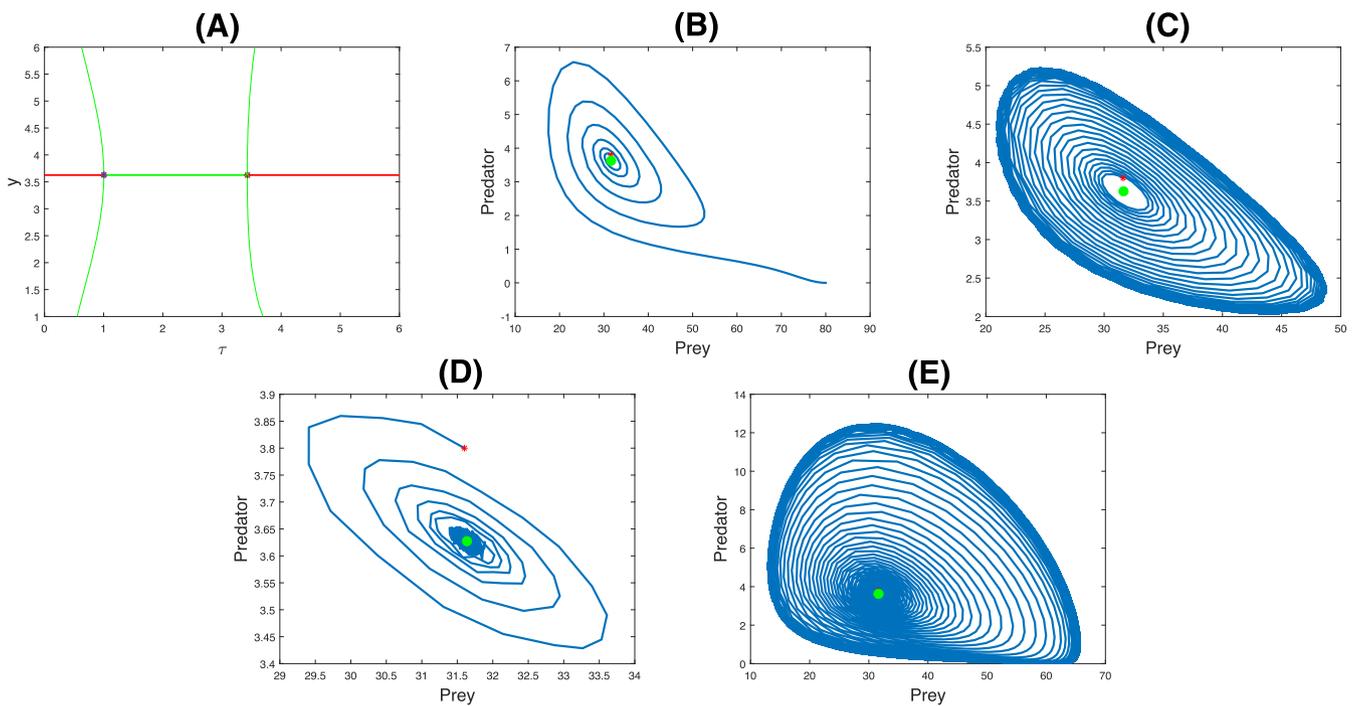
FIGURE 7 (A) Bifurcation diagram with respect to predator when time delay varies. For initial conditions (31.6, 3.8) (indicated by red dot), the phase portrait is plotted for (B) $\tau = 0.3$, (C) $\tau = 0.8$, (D) $\tau = 2$, and (E) $\tau = 5$, where $r = 1.2$, $K = 80$, $\alpha = 0.2$, $\beta = 0.1$, $m = 2.0$, $C = 2.1$, $\gamma = 0.001$. Here, the green dot indicates the equilibrium (31.6361, 3.6272) [Colour figure can be viewed at wileyonlinelibrary.com]

We also provide an example below where instead of appearance of two consecutive τ_j^+, ($j = 0, 1$), we have appearance of four consecutive τ_j^+, ($j = 0, 1, 2, 3$), before the appearance of the first τ_0^-.

Example 4.7. We take the parameter set as $r = 0.4$, $K = 100$, $\alpha = 1$, $\beta = 0.9$, $\gamma = 0.8$, $m = 0.1$, and $C = 16.9$. Two interior equilibria are $E_1 = (21.3842, 0.3144)$ and $E_2 = (94.0497, 0.0238)$. The equilibrium E_1 is unstable focus in the absence of τ, since $a_1 + a_2 = -0.0080 < 0$ and $a_3 + a_4 = 0.1026 > 0$. At E_1, $a_3^2 - a_4^2 = 0.000064$, $a_2^2 - a_1^2 + 2a_3 = 0.1143$, and $(a_2^2 - a_1^2 + 2a_3)^2 - 4(a_3^2 - a_4^2) = 0.0128$. Thus, the conditions mentioned in **Case 4** are met here. These conditions lead to $\omega_+ = 0.3373$ and $\omega_- = 0.0238$. The values of critical time delays are supplied in Table 5. However, it can be seen from the table, that the appearance of two consecutive τ_0^+ and τ_1^+ never makes the equilibrium E_1 stable. Hence, instability persists for all time delay around E_1.

Now, for the equilibrium E_2, we have $a_1 + a_2 = 0.2764$ and $a_3 + a_4 = -0.0347$, which indicate E_2 to be a saddle point when $\tau = 0$. As quoted in Theorem 4.7, the equilibrium E_2 could not alter its stability.

4.5 | Instability switching

Here validity of Theorem 4.6 for system (4) is demonstrated through the following example.

Example 4.8. We consider the parameter set as $r = 1.2$, $K = 80$, $\alpha = 0.2$, $\beta = 0.1$, $\gamma = 0.001$, $m = 2.0$, and $C = 2.1$. We determine two interior equilibria $E_1 = (31.6361, 3.6272)$ and $E_2 = (68.4297, 0.8677)$. Now, $a_1 + a_2 = -0.2564$ and $a_3 + a_4 = 1.1066$, when evaluated at E_1. We can conclude that, in absence of time delay, the interior equilibrium E_1 is unstable. Further, $a_3^2 - a_4^2$, $a_2^2 - a_1^2 + 2a_3$, and $(a_2^2 - a_1^2 + 2a_3)^2 - 4(a_3^2 - a_4^2)$ are found to be 0.8836, 3.2440 and 6.9891 respectively. Table 6 gives the values of the critical time delays, which can be arranged in ascending order as follows

$$\tau_0^- < \tau_0^+ < \tau_1^+ < \tau_2^+ < \tau_1^- < \tau_3^+ < \tau_4^+ < \tau_5^+ < \tau_2^- < \ldots .$$

Since two consecutive τ_j^+ ($j = 0, 1, 2$) appear successively, so by Theorem 4.6, we conclude that the interior equilibrium E_1 undergoes instability switching. The bifurcation diagram and phase portraits are shown in Figure 7. For the equilibrium E_2, we get $a_1 + a_2 = -0.3885$ and $a_3 + a_4 = -1.1051$. Thus, the equilibrium E_2 is a saddle and remains saddle for all time delay as mentioned in Theorem 4.7.

5 | CONCLUSION

In this paper, we considered a predator-prey system with Holling type I functional response and intra-specific competition among the predators, but the numerical response is not proportional to the functional response. The role of such a unbalanced functional and numerical responses has been studied by a limited number of researchers to explore population dynamics in the contexts of Allee induced dynamics[1,34] biological pest control,[35] and hydra effect.[36] A special feature of our model is that the number of coexisting equilibria (if exist) is always two. We investigated the model dynamics under varying time delay. We have shown the positivity and boundedness of the solutions to the delayed model. The trivial equilibrium is always unstable, whereas the boundary equilibrium is locally stable even in the presence of the pair of coexisting equilibria. Local dynamics of the trivial and boundary equilibrium is independent of time delay. We have proved the global stability of the boundary equilibrium. Because of the existence of two interior equilibria, global stability at coexisting equilibrium does not hold neither in the delayed nor in non-delayed system.

We examined the change of stability of the coexisting equilibria. We have presented four cases (**Cases 1–4**) for the existence of a pair of purely imaginary eigenvalues of the characteristic equation for some critical time delays. A series of theorems (Theorem 4.2–4.7) are sorted out based on the discussion of the four **Cases 1–4**. Applicability of all the theorems in our model are validated with suitable examples. The interesting outcomes of the local dynamics corresponding to one of the coexisting equilibria (which is not the saddle equilibrium) are as follows:

(i) The equilibrium does not change in stability with increase in time delay.
(ii) The equilibrium undergoes stability change (from stable to unstable).
(iii) The equilibrium undergoes one or multiple stability switching.
(iv) The equilibrium undergoes instability switching.
(v) The equilibrium does not change instability.

All the above situations were explained numerically as well as graphically. Toaha[32] proved that at most two outcomes **R1** and **R2** are possible when the model does not involve the intraspecific competition among predators, and both the functional and numerical responses are of Holling type I. We arrived at the same conclusion with Toaha[32] when the intraspecific competition is present among predators (analytical proof is given in Appendix A1). Therefore, we conclude that the variety of such delay-induced dynamical behaviors in a single and relatively simple model are due to the presence of the distinct numerical response function. This is one of the novelties in our work.

While exploring the delay-induced dynamics, we identified some interesting facts which could be worth-mentioning both from mathematical and computational view points. Several earlier contributions highlighted that stability remains unaltered due to varying delay if no ω exists from the corresponding characteristic equation. Nevertheless, existence of a ω leads to stability change, and existence of two values of ω result to stability switching. However, corresponding to one of the equilbrium E_1, we detected situation where two ω exist, but the equilibrium undorgoes stability change only (Example 4.3). Apart from the results **R1**–**R4**, more complicated and rich analysis appeared in this model. Therefore, a detailed analysis is essential while investigating a delayed population model.

In Theorem 4.7, we have proved that a saddle equilibrium does not change its stability due to varying delay. A detailed mechanism, associated with the stability of the saddle point, has been explained numerically and graphically. In all the examples, ω exists, but the transversality condition $\left[\frac{d(\text{Re}\lambda)}{d\tau}\right]_{\tau=\tau_j^+} > 0$ holds at each critical delays. Graphical representation demonstrate the mechanism of creating new eigenvalues of the characteristic function only in $\mathbb{C}^-$ plane, while increase of eigenvalues in $\mathbb{C}^+$ is possible due to the crossing of eigenvalues from $\mathbb{C}^-$ to $\mathbb{C}^+$ through $\mathbb{C}^0$. This knowledge and information might be useful to study many more delay differential equations.

In the current study, we examined the stability of two coexisting equilibria. The two coexisting equilibria exists due to the presence of Allee effect in the model. However, several stage-structured ecological systems exhibit multi-stability at equilibria. It could be interesting to address non delayed systems which possesses such multi-stability and examine how multi-stability could be altered due to delays.

ACKNOWLEDGEMENT

CONFLICT OF INTEREST

This work does not have any conflict of interest.

ORCID

Bapan Ghosh 🔟 https://orcid.org/0000-0002-5006-2440

REFERENCES

1. Verdy A. Modulation of predator-prey interactions by the Allee effect. *Ecolog Modell*. 2010;221(8):1098-1107.
2. Kuperman MN, Abramson G. Allee effect in models of interacting species. *Chaos, Solitons Fract*. 2021;153:111512.
3. Přibylová L, Berec L. Predator interference and stability of predator-prey dynamics. *J Math Biol*. 2015;71(2):301-323.
4. Berec L. Impacts of foraging facilitation among predators on predator-prey dynamics. *Bull Math Biol*. 2010;72(1):94-121.
5. Liu W, Jiang Y. Bifurcation of a delayed Gause predator-prey model with Michaelis-Menten type harvesting. *J Theoret Biol*. 2018;438:116-132.
6. Meng X-Y, Li J. Dynamical behavior of a delayed prey-predator-scavenger system with fear effect and linear harvesting. *Int J Biomath*. 2021;14(4):2150024.
7. Barman B, Ghosh B. Role of time delay and harvesting in some predator-prey communities with different functional responses and intra-species competition. *Int J Modell Simul*. 2022;42(6):883-901. doi:10.1080/02286203.2021.1983747
8. Rihan FA, Rajivganthi C. Dynamics of fractional-order delay differential model of prey-predator system with Holling type III and infection among predators. *Chaos, Solitons Fract*. 2020;141:110365.
9. Li Y, Liu H, Yang R. Time-delay effect on a diffusive predator-prey model with habitat complexity. *Adv Differ Equ*. 2021;2021(1):1-24.
10. Ghasemabadi A, Rahmani Doust MH. Hopf bifurcation and stability analysis of delayed Lotka-Volterra predator-prey model having disease for both existing species. *New Trends in Applied Analysis and Computational Mathematics*. Springer; 2021:155-166.
11. Dubey B, Kumar A. Dynamics of prey-predator model with stage structure in prey including maturation and gestation delays. *Nonlin Dyn*. 2019;96(4):2653-2679.
12. Alidousti J, Ghahfarokhi MM. Stability and bifurcation for time delay fractional predator-prey system by incorporating the dispersal of prey. *Appl Math Modell*. 2019;72:385-402.
13. Kar TK, Matsuda H. Controllability of a harvested prey-predator system with time delay. *J Biolog Syst*. 2006;14(2):243-254.
14. Li H, Takeuchi Y. Dynamics of the density dependent predator–prey system with Beddington-DeAngelis functional response. *J Math Anal Appl*. 2011;374(2):644-654.
15. Barman B, Ghosh B. Dynamics of a spatially coupled model with delayed prey dispersal. *Int J Modell Simul*. 2022;42(3):400-414.
16. Collera JA. Bifurcations in delayed Lotka-Volterra intraguild predation model. *J Math Soc Philipp*. 2014;37:11-22.
17. Rabago JFT, Collera JA. Hopf bifurcation in a delayed intraguild predation model. *Southeast Asian Bull Math*. 2018;42(5):691-709.
18. Zhang X, Shi R, Yang R, Wei Z. Dynamical behaviors of a delayed prey-predator model with Beddington-DeAngelis functional response: Stability and periodicity. *Int J Bifurcation Chaos*. 2020;30(16):2050244.
19. Jiang Z, Wang L. Global Hopf bifurcation for a predator-prey system with three delays. *Int J Bifurcation Chaos*. 2017;27(7):1750108.
20. Pati NC, Ghosh B. Delayed carrying capacity induced subcritical and supercritical Hopf bifurcations in a predator-prey system. *Math Comput Simul*. 2022;195:171-196.

21. Singh A, Parwaliya A, Kumar A. Hopf bifurcation and global stability of density-dependent model with discrete delays involving Beddington-DeAngelis functional response. *Math Methods Appl Sci*. 2021;44(11):8838-8861.

22. Panday P, Samanta S, Pal N, Chattopadhyay J. Delay induced multiple stability switch and chaos in a predator–prey model with fear effect. *Math Comput Simul*. 2020;172:134-158.

23. Kumar R, Sharma AK. Stability and Hopf bifurcation analysis of a delayed innovation diffusion model with intra-specific competition. *Int J Bifurcation Chaos*. 2021;31(14):2150213.

24. Drake JM, Kramer AM. Allee effects. *Nat Educ Knowl*. 2011;3(10):2.

25. Zu J, Mimura M. The impact of Allee effect on a predator–prey system with Holling type II functional response. *Appl Math Comput*. 2010;217(7):3542-3556.

26. Anacleto M, Vidal C. Dynamics of a delayed predator-prey model with Allee effect and Holling type II functional response. *Math Methods Appl Sci*. 2020;43(9):5708-5728.

27. Xiao Z, Xie X, Xue Y. Stability and bifurcation in Holling type II predator-prey model with Allee effect and time delay. *Adv Differ Equ*. 2018;2018(1):1-21.

28. Vinoth S, Sivasamy R, Sathiyanathan K, et al. Dynamical analysis of a delayed food chain model with additive Allee effect. *Adv Differ Equ*. 2021;2021(1):1-20.

29. Tao X, Zhu L. Study of periodic diffusion and time delay induced spatiotemporal patterns in a predator-prey system. *Chaos, Solitons Fract*. 2021;150:111101.

30. Wangersky PJ, Cunningham WJ. Time lag in prey-predator population models. *Ecology*. 1957;38(1):136-139.

31. Martin A, Ruan S. Predator-prey models with delay and prey harvesting. *J Math Biol*. 2001;43(3):247-267.

32. Toaha S. Stability analysis of Wangersky-Cunningham model with constant effort of harvesting. *Jurnal Matematika, Statistika dan Komputasi*. 2018;12(2):140-152.

33. Ye Y, Liu H, Wei Y, Ma M, Zhang K. Dynamic study of a predator-prey model with weak Allee effect and delay. *Adv Math Phys*. 2019;2019:1-15.

34. Zhou S-R, Liu Y-F, Wang G. The stability of predator-prey systems subject to the Allee effects. *Theoret Popul Biol*. 2005;67(1):23-31.

35. Bajeux N, Grognard F, Mailleret L. Augmentative biocontrol when natural enemies are subject to Allee effects. *J Math Biol*. 2017;74(7):1561-1587.

36. Costa MIS, dos Anjos L. Multiple hydra effect in a predator-prey model with Allee effect and mutual interference in the predator. *Ecolog Modell*. 2018;373:22-24.

37. Costa MIS, Esteves PV, Faria LDB, dos Anjos L. Prey dynamics under generalist predator culling in stage structured models. *Math Biosci*. 2017;285:68-74.

38. Shu H, Hu X, Wang L, Watmough J. Delay induced stability switch, multitype bistability and chaos in an intraguild predation model. *J Math Biol*. 2015;71(6-7):1269-1298.

39. Kang Y, Wedekin L. Dynamics of a intraguild predation model with generalist or specialist predator. *J Math Biol*. 2013;67(5):1227-1259.

40. Cooke KL, Grossman Z. Discrete delay, distributed delay and stability switches. *J Math Anal Appl*. 1982;86(2):592-627.

APPENDIX A: DYNAMICS OF WC MODEL WITH INTRA-SPECIFIC COMPETITION

We recall the system (3) considered in Section 2. As obtained in Section 4, the equilibrium points for system (3) are (i) the trivial equilibrium $(0, 0)$, (ii) the boundary equilibrium $(K, 0)$, and (iii) the interior equilibrium $(x^*, y^*) = \left(K - K\alpha \frac{\beta K - m}{\beta K \alpha + \gamma r}, \frac{r(\beta K - m)}{\beta K \alpha + \gamma r} \right)$, which exists only if $\beta K > m$.

Linearizing system (3) around the interior equilibrium, we get

$$\dot{x}(t) = \left(r - \frac{2rx^*}{K} - \alpha y^* \right) x(t) - \alpha x^* y(t), \tag{A1}$$

$$\dot{y}(t) = -(m + 2\gamma y^*) y(t) + \beta y^* x(t - \tau) + \beta x^* y(t - \tau). \tag{A2}$$

The characteristic equation is given as

$$\lambda^2 + a_1 \lambda + a_2 \lambda e^{-\lambda \tau} + a_3 + a_4 e^{-\lambda \tau} = 0, \tag{A3}$$

where

$$a_1 = \frac{rx^*}{K} + m + 2\gamma y^*,$$

$$a_2 = -\beta x^*,$$

$$a_3 = r\frac{x^*}{K}(m + 2\gamma y^*),$$

$$a_4 = -r\beta x^*\frac{x^*}{K} + \alpha\beta x^* y^*.$$

For $\tau = 0$, the characteristic equation reduces to

$$\lambda^2 + (a_1 + a_2)\lambda + (a_3 + a_4) = 0. \tag{A4}$$

Since $\beta K > m$ holds for the existence of equilibrium, therefore,

$$a_1 + a_2 = \frac{r(\alpha m + \gamma r) + \gamma r(K\beta - m)}{K\alpha\beta + \gamma r} > 0,$$

and

$$a_3 + a_4 = \frac{r(\alpha m + \gamma r)(K\beta - m)}{K\alpha\beta + \gamma r} > 0.$$

So we can conclude that, system (3) is stable when $\tau = 0$.

Now we want to verify if there exist roots $\lambda = \pm i\omega$, $(\omega > 0)$ of the characteristic equation (A3) when τ increases. Substituting $\lambda = i\omega$ in equation (A3) and separating the real and imaginary parts, we obtain

$$-\omega^2 + a_2\omega \sin \omega\tau + a_4 \cos \omega\tau + a_3 = 0, \tag{A5}$$

$$a_1\omega + a_2\omega \cos \omega\tau - a_4 \sin \omega\tau = 0. \tag{A6}$$

Eliminating τ from equations (A5) and (A6), we get

$$(\omega^2 - a_3)^2 + a_1^2\omega^2 = a_2^2\omega^2 + a + 4^2,$$

which reduces to

$$\omega^4 + (a_1^2 - a_2^2 - 2a_3)\omega^2 - a_4^2 + a_3^2 = 0. \tag{A7}$$

The roots of equation (A7) are

$$\omega_\pm^2 = \frac{1}{2}(a_2^2 - a_1^2 + 2a_3) \pm \frac{1}{2}\left[(a_2^2 - a_1^2 + 2a_3)^2 - 4(a_3^2 - a_4^2)\right]^{1/2}. \tag{A8}$$

We analyze the stability of system (3) based on the roots of equation (A7).

We find that

$$(a_2^2 - a_1^2 + 2a_3) = -\frac{r^2(\alpha m + \gamma r)^2 + \gamma^2 r^2(K\beta - m)^2 + 2K\beta\gamma r(K\beta - m)(\alpha m + \gamma r)}{(K\alpha\beta + \gamma r)^2} < 0,$$

which implies that two positive $\omega_\pm^2$ is not possible to obtain. Thus, there does not exist stability switching for system (3).